

Radiosynthesis and biological evaluation of ^{123}I -(\pm)-trans-2-hydroxy-5-((E)-3-(iodo)allyloxy)-3-(4-phenyl-1-piperazinyl) tetralin

Thaer Assaad,
Abdul H. Al Rayyes

Abstract. This work reports both the radiolabeling and preliminary biodistribution results in the rat brains of (\pm)- ^{123}I -II. The novel benzovesamicol derivative (\pm)- ^{123}I -II was successfully labeled with iodine-123 from its corresponding n-tributyltin, with radiochemical purity greater than 97% and radiochemical yield in the range 50–55%. (\pm)- ^{123}I -II showed a higher accumulation in striatum than in the other regions studied. To determine if (\pm)- ^{123}I -II could provide an advantage compared to reference compound [^{125}I]-IBVM a kinetic study was carried out, at each point of the kinetic study, (\pm)- ^{123}I -II showed a lower specific binding compared to [^{125}I]-IBVM. Time activity curves of (\pm)- ^{123}I -II confirmed that this compound is inferior to [^{125}I]-IBVM to explore the VAcHT *in vivo* by SPECT. Moreover, it is well known that interaction at the VAcHT binding site is enantioselective, and therefore, working with enantiomerically pure compounds, could improve the compound activity.

Key words: Alzheimer's disease • brain biodistribution • injected dose (ID) • radioiodination • vesamicol derivatives • vesicular acetylcholine transporter (VAcHT)

Introduction

Alzheimer's disease is one of the most frequent human neurodegenerative diseases. One of the characteristics occur early in this disease is the degeneration of cholinergic neurons of the basal forebrain [3]. Recently, considerable effort has been devoted to the development of single photon emission computed tomography (SPECT) and positron emission tomography (PET) radioligands suitable for *in vivo* monitoring of these cholinergic deficits. Consequently, several labeled vesamicol derivatives have been developed, [6, 7, 11] such as benzovesamicols (-)-5-iodobenzovesamicol, ^{123}I -IBVM [7] (-)-(^{11}C)-5-*N*-methylamino benzovesamicol (^{11}C)-MABV [9] (-)-(^{18}F)-fluoroethoxybenzovesamicol (^{18}F)-FEOBV [10] (E)-(R,R)-2-hydroxy-5-(3-iodoprop-2-en-1-oxy)-3-(4-phenylpiperidino)tetralin, (R,R)-5-AOIB and fluoropropoxy benzovesamicol (^{18}F)-FPOBV [15]. It has been reported that the piperidine represents the main part of the benzovesamicol, which determines the affinity of benzovesamicol receptor on vesicular acetylcholine transporter (VAcHT) [12]. Bando *et al.* [4] showed that the replacement of the piperidine ring in the structure of IBVM with a piperazine ring resulted in the formation of DRC140 derivative (Fig. 1), a compound of high affinity and

T. Assaad[✉], A. H. Al Rayyes
Cyclotron Division,
Chemistry Department,
Atomic Energy Commission of Syria,
Damascus, P. O. Box 6091, Syrian Arab Republic,
Tel.: +963 11 213 2580, Fax: +963 11 611 2289,
E-mail: cscientific@aec.org.sy

Received: 16 March 2011

Accepted: 22 June 2011

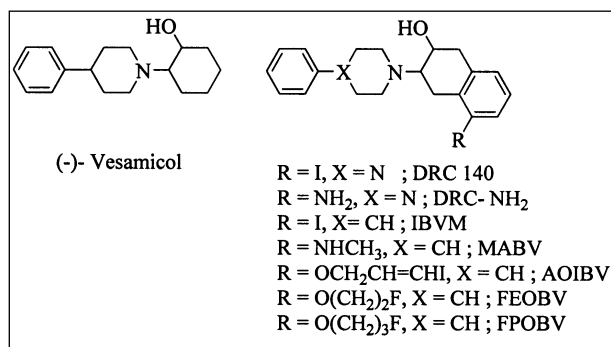


Fig. 1. Vesamicol analogues.

selectivity for the VACHT over σ_1 and σ_2 receptors. To date, however, only few studies in humans have been reported with these tracers. This may be due to the unfavorable pharmacokinetic properties of these highly lipophilic compounds and to their potential toxicity [8, 13, 14].

In our continuing effort to map the VACHT and to develop more potent and selective radiotracers for studying the cholinergic system *in vivo*, we have recently reported the synthesis of the (\pm)-trans-2-hydroxy-5-((E)-3-(iodo)allyloxy)-3-(4-phenyl-1-piperazinyl) tetralin derivative [1]. As this derivative displays calculated lipophilicity (4.87) which is slightly different from reference compound IBVM (5.15), we have evaluated the *in vivo* behavior of this compound and compared it with IBVM.

Experimental

General remarks

All chemical reagents and solvents were of commercial quality and used as received. [¹²⁵I]-IBVM was prepared following a reported procedure by iododestannylation of its n-tributyltin precursor, synthesized as previously described [13, 15]. High-purity iodide-123 has been produced by proton irradiation of enriched xenon-124 target having a minimal concentration of xenon-124 of 98% inside KIPROS 50 target (Karlsruhe iodine production system). The nuclear reaction was induced using 30 MeV proton beam. The 30 MeV proton beam is extracted from a Cyclone-30 cyclotron for ion beam applications (IBA). ¹²³Ina has been produced using a KIPROS concentration and purification unit. The paper chromatographic analysis was performed using Whatman 3MM paper chromatography strips (2 × 10 cm). The radioactive spot migration was determined by a gamma scanner purchased from Bioscan equipped by a sodium iodide detector.

Radiolabeling procedure of [¹²³I]-(\pm)-trans-2-hydroxy-5-((E)-3-(iodo)allyloxy)-3-(4-phenyl-1-piperazinyl) tetralin (\pm)-[¹²³I]-II

(\pm)-[¹²³I]-II compound was prepared using electrophilic radioiododestannylation of the tri-n-butyltin precursors (\pm)-I, with some modifications to the described proce-

dures [5, 15]. Briefly, 210 μ l of 0.02 N ethanolic H₂SO₄ was added to a vial containing 41.81 MBq (1.127 mCi) of Na¹²³I in 20 μ l of 0.02 N NaOH, followed by a tin precursor (125 μ g in 125 μ l of EtOH). The pH of the reaction mixture was monitored (pH = 0–1), and the reaction was initiated by the addition of 50 μ l of freshly prepared aqueous Chloramine-T trihydrate (15 mg/ml), followed by vigorous shaking for 2 min. Another, 50 μ l of freshly prepared aqueous Chloramine-T trihydrate (15 mg/ml) was added again, followed by vigorous shaking for a further 2 min. The reaction was quenched by the addition of 420 μ l of 0.02 N aqueous NH₄OH.

Purification procedure

The free ¹²³I was eliminated by passing the reaction mixture through a modified ionic exchange column 2 × 10 mm which contained a Biorex resin (200–400 mesh). The labeled product (\pm)-[¹²³I]-II was then concentrated and washed using a C-18 Sep-Pak column, and eluted subsequently from the C-18 Sep-Pak with 2 ml of EtOH abs. Finally, this solution was diluted with 0.9% normal saline. Radiochemical purity was determined by paper chromatography using ammonium acetate/ethanol 95% (1/1) as elution solution. The strips were scanned by the gamma scanner after the separation process.

Cerebral biodistribution studies in rats

Male 2-month-old Wistar han rats (175–250 g) were used in the experiments. Each rat received an intravenous injection of 1.85–2.59 MBq of (\pm)-[¹²³I]-II (via the tail vein) in 0.3 ml solution of 0.9% NaCl/EtOH, under ethoxy ethane anesthesia. All animals were sacrificed 2 h post injection of the radioactive compound. The brain was removed, and samples of the cerebellum (cereb), striatum (str), frontal cortex (ctx), and hippocampus (hippo) were dissected and weighed. The radioactivity of each sample was measured in a GAMMA MÜVEK NK-360 counter. Results were expressed as mean percentage of the injected dose per gram (%ID/g) tissue \pm standard deviation (SD) (12 rats) (Fig. 2). In order to evaluate *in vivo* deiodination of (\pm)-[¹²³I]-II, we removed the thyroid gland of each animal and measured its radioactivity. This radioactivity remained constant at low level for each sampling time.

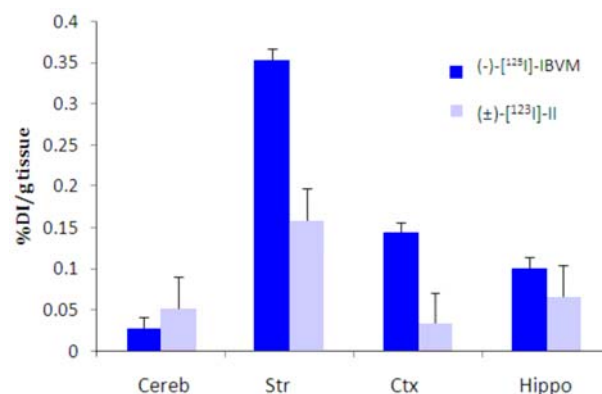


Fig. 2. Cerebral biodistribution of (\pm)-[¹²³I]-II, (-)-[¹²⁵I]-IBVM in the rat.

Cerebral kinetic studies in rats

For kinetic studies, rats received an intravenous injection of (\pm)- ^{123}I -II or (-)- ^{125}I -IBVM (1 MBq in 250 μl of EtOH/saline 20/80) and were sacrificed 30 min, 1 or 2 h post injection ($n = 4$ rats per group). Samples of blood and cerebral regions (cerebellum, striatum, frontal cortex and hippocampus) were removed and weighed, and their radioactivities were measured. The uptake was expressed as the (%ID/g) of tissue. To evaluate *in vivo* deiodination of tracers, the entire thyroid gland of each animal was removed and its radioactivity was measured.

Result and dissection

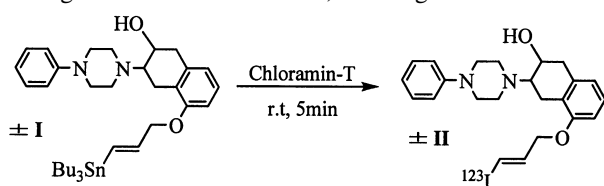
Radiochemistry

Target compound of ^{123}I -(\pm)-trans-2-hydroxy-5-((E)-3-(iodo)allyloxy)-3-(4-phenyl-1-piperazinyl) tetralin (\pm)- ^{123}I -II (Scheme 1), was prepared using its corresponding n-tributyltin precursor (\pm)-I as a racemic mixture, which was synthesized as previously described from (\pm)-7-(4-phenylpiperazin-1-yl)-5,6,7,8-tetrahydronaphthalene-1,6-diol [1, 2, 4–12, 15]. The reaction was carried out at room temperature with Chloramine-T as the oxidant. Radiolabeled compound was obtained with radiochemical purity greater than 97% and in radiochemical yields in the range 50–55%.

Cerebral biodistribution studies in rats

Cerebral biodistribution of (\pm)- ^{123}I -II was studied in rats and the results were compared to those obtained with ^{125}I -IBVM (Fig. 2). Two hours post injection (\pm)- ^{123}I -II showed a higher accumulation in striatum than in the other regions studied. The striatal binding was found to be higher by a factor of 2.4, 3.09 and 4.93 compared to those of hippocampus, cerebellum and cortex, respectively. The high uptake of (\pm)- ^{123}I -II in striatum could be associated with VAcHT binding. By contrast, the high concentration found in the cerebellum could be associated with non-specific binding to the VAcHT.

In similar experimental conditions, the reference compound (-)- ^{125}I -IBVM showed a lower accumulation in the cerebellum (representing the non-specific binding) than in the other regions studied with region/cerebellum ratios of 13, 5.29 and 3.7 for the striatum, frontal cortex and hippocampus, respectively (Fig. 3). The cerebral biodistribution of (-)- ^{125}I -IBVM, has shown a different profile compared to (\pm)- ^{123}I -II. However, the uptake in the cerebellum, which could be considered as non-specific binding, was twice (1.9) as high as for IBVM. Thus, the regions of interest



Scheme 1. Radio syntheses of (\pm)- ^{123}I -II.

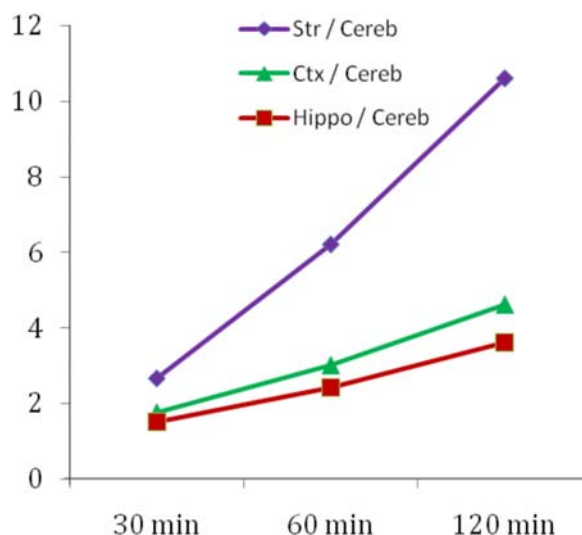


Fig. 3. Time-activity curves of (\pm)- ^{123}I -II in the rat brain.

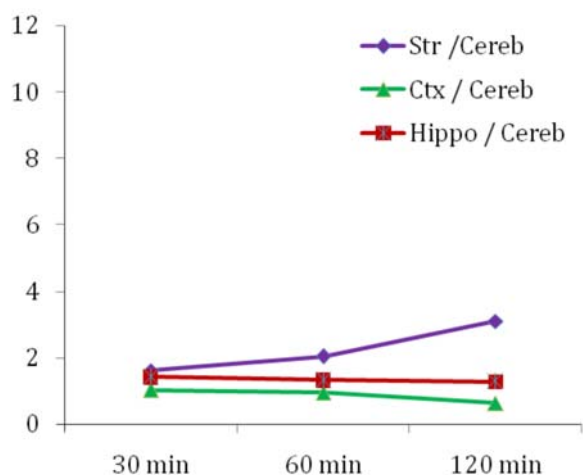


Fig. 4. Time-activity curves of (-)- ^{125}I -IBVM in the rat brain.

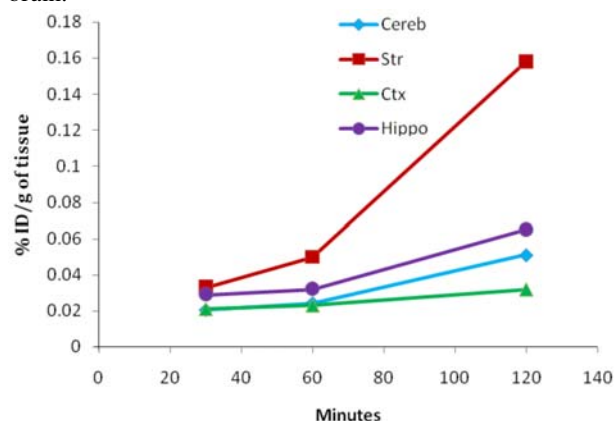


Fig. 5. Kinetic study of (\pm)- ^{123}I -II in the rat brain.

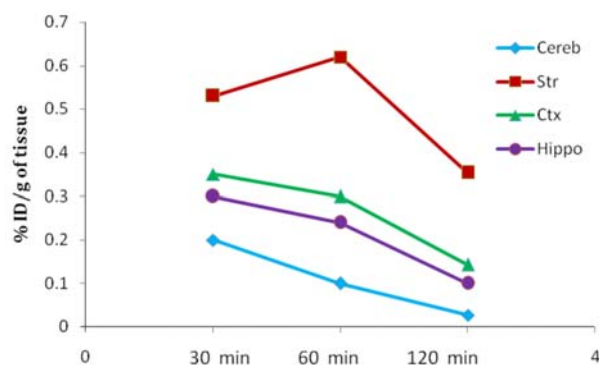
(ROIs)/cerebellum ratios, which characterize the specific binding, were higher for IBVM compared to (\pm)- ^{123}I -II (Figs. 4 and 5, Table 1) with a maximum striatum/cerebellum ratio of 13 for IBVM vs. 3.09 for (\pm)- ^{123}I -II.

Cerebral kinetic studies in rats

Figure 6 represents time activity curves (TACs) of brain areas with different expression levels of VAcHT. TACs

Table 1. Distribution (%/ID/g of tissue \pm SD) of (\pm)-[¹²³I]-II and [¹²⁵I]-IBVM in the rat brain

	(%/ID/g) of (\pm)-[¹²³ I]-II			(%/ID/g) of [¹²⁵ I]-IBVM		
	30 min	60 min	120 min	30 min	60 min	120 min
Cerebellum	0.020 \pm 0.016	0.024 \pm 0.006	0.051 \pm 0.013	0.20 \pm 0.02	0.10 \pm 0.01	0.027 \pm 0.01
Striatum	0.033 \pm 0.067	0.049 \pm 0.02	0.158 \pm 0.038	0.53 \pm 0.10	0.62 \pm 0.01	0.353 \pm 0.05
Cortex	0.021 \pm 0.005	0.023 \pm 0.008	0.032 \pm 0.002	0.35 \pm 0.08	0.30 \pm 0.01	0.143 \pm 0.04
Hippocampus	0.029 \pm 0.019	0.032 \pm 0.011	0.065 \pm 0.008	0.30 \pm 0.02	0.24 \pm 0.01	0.100 \pm 0.01
Thyroid	0.033 \pm 0.011	0.067 \pm 0.02	0.114 \pm 0.078	0.09 \pm 0.008	0.12 \pm 0.012	0.190 \pm 0.03

**Fig. 6.** Kinetic study of (-)-[¹²⁵I]-IBVM in the rat brain.

of (\pm)-[¹²³I]-II showed that the highest accumulations was in the striatum followed by the hippocampus, cerebellum and then the cortex, while the reference compound showed that the highest accumulations was in the striatum (brain area with high VACHT density) followed by the cortex, hippocampus and then the cerebellum, which was used as a reference area (low VACHT density). TACs of (\pm)-[¹²³I]-II increased continuously for all brain areas, while the striatal TACs were stable from 30 min to 2 h post injection for (-)-[¹²⁵I]-IBVM and decreased continuously for the cortex, hippocampus and cerebellum. This characteristic makes the specific binding value (radioactivity ratio between the brain area of interest and cerebellum) increasing over time for both compounds except for the cortex and hippocampus values in (\pm)-[¹²³I]-II. However, when compared both compounds, (-)-[¹²⁵I]-IBVM clearly showed a better *in vivo* profile since it crossed the blood-brain barrier in much easier way (0.62 \pm 0.1% ID/g tissue 1 h post injection), compared to 0.049% ID/g tissue for (\pm)-[¹²³I]-II. The specific binding in striatum (striatum/cerebellum) for (-)-[¹²⁵I]-IBVM was 2.65 30 min post injection and increased to 13 2 h post injection when (\pm)-[¹²³I]-II showed its highest value of 3.09 2 h post injection.

Thyroid radioactivity was expressed as the percentage of injected dose per whole gland (%/ID/g) as the weight of this gland is difficult to measure with precision. For both tracers, a gradual increase of radioactivity during time was observed in the thyroid. However, this accumulation was less for (\pm)-[¹²³I]-II (0.033, 0.067 and 0.11% ID at 30 min, 1 and 2 h, respectively) compared to (-)-[¹²⁵I]-IBVM (0.09, 0.12 and 0.19% ID at 30 min, 1 and 2 h, respectively) at each point of the study.

Conclusion

A vesamicol analog as ligand for the VACHT was developed and evaluated in the brain of rats. Biodistribution studies showed a good brain penetration of (\pm)-[¹²³I]-II.

A higher level of (\pm)-[¹²³I]-II was found in striatum than in the other regions studied. However, when compared to (-)-[¹²⁵I]-IBVM, (\pm)-[¹²³I]-II showed lower specific binding in all brain areas explored 2 h post injection. To determine if (\pm)-[¹²³I]-II could provide an advantage compared to [¹²⁵I]-IBVM, a kinetic study was realized. Even if time activity curves of (\pm)-[¹²³I]-II confirmed that this compound could not be used to visualize the VACHT *in vivo*, at each point of the kinetic study, (\pm)-[¹²³I]-II showed a lower specific binding compared to (-)-[¹²⁵I]-IBVM. All these results make (\pm)-[¹²³I]-II inferior to IBVM, which remains the standard tracer to explore the VACHT *in vivo* by SPECT. Although it is well known that the interaction at the VACHT binding site is stereoselective, only racemic mixtures have been used. We can expect that enantiomeric separation of (\pm)-[¹²³I]-II could provide compounds with improved results.

Acknowledgment. The authors thank Prof. I. Othman, Director General of AECS and Prof. T. Yassine, head of the Department of Chemistry for their support and encouragement. Thanks are also due to Mr. E. Ghanem, for his assistance with the preparation of compounds and biodistribution study. We also thank R. Ajaya, N. Karajoli, A. Shraibati and O. Hafez for their assistance with some of the laboratory work.

References

- Assaad T (2011) Synthesis and characterization of novel benzovesamicol analogs. *Turk J Chem* 35:189–200
- Assaad T, Mavel S, Emond P *et al.* (2007) Synthesis and *ex vivo* evaluation of aza-trozamicol analogs as SPECT radiotracers for exploration of the vesicular acetylcholine transporter. *J Labelled Compd Radiopharm* 50:139–14
- Auld DS, Kornecook TJ, Bastianetto S, Quirion R (2002) Alzheimer's disease and the basal forebrain cholinergic system: relations to beta-amyloid peptides, cognition, and treatment strategies. *Prog Neurobiol* 68:209–245
- Bando K, Naganuma T, Taguchi K *et al.* (2000) Piperazine analog of vesamicol: *in vitro* and *in vivo* characterization for vesicular acetylcholine transporter. *Synapse* 38:27–37
- Emond P, Mavel S, Zea-Ponce Y *et al.* (2007) (E)-[¹²⁵I]-5-AOIBV: a SPECT radioligand for the vesicular acetylcholine transporter. *Nucl Med Biol* 34:967–971
- Jung YW, Frey KA, Mulholland GK *et al.* (1996) Vesamicol receptor mapping of brain cholinergic neurons with radioiodine-labeled positional isomers of benzovesamicol. *J Med Chem* 39:3331–3342
- Jung YW, Van Dort ME, Gildersleeve DL, Wieland DM (1990) A radiotracer for mapping cholinergic neurons of the brain. *J Med Chem* 33:2065–2068
- Kuhl DE, Minoshima S, Fessler JA *et al.* (1996) *In vivo* mapping of cholinergic terminals in normal aging,

- Alzheimer's disease, and Parkinson's disease. *Ann Neurol* 40:399–410
- Mulholland GK, Jung YW (1992) Improved synthesis of [^{11}C]methylamino-benzovesamicol. *J Labelled Compd Radiopharm* 31:253–259
 - Mulholland GK, Jung YW, Wieland DM, Kilbourn MR, Kuhl DE (1993) Synthesis of [^{18}F]-fluoroethoxybenzovesamicol, a radiotracer for cholinergic neurons. *J Labelled Compd Radiopharm* 33:589–591
 - Parsons SM, Bahr BA, Rogers GA, Clarkson ED, Noremborg K, Hicks BW (1993) Acetylcholine transporter-vesamicol receptor pharmacology and structure. *Prog Brain Res* 98:175–181
 - Rogers GA, Parsons SM, Anderson DC *et al.* (1989) Synthesis, *in vitro* acetylcholine-storage-blocking activities, and biological properties of derivatives and analogues of trans-2-(4-phenylpiperidino)cyclohexanol (vesamicol). *J Med Chem* 32:1217–1230
 - Sorger D, Schliebs R, Kampfer I *et al.* (2000) *In vivo* [^{125}I]-iodobenzovesamicol binding reflects cortical cholinergic deficiency induced by specific immunolesion of rat basal forebrain cholinergic system. *Nucl Med Biol* 27:23–31
 - Van Dort ME, Jung YW, Gildersleeve DL, Hagen CA, Kuhl DE, Wieland DM (1993) Synthesis of the ^{123}I - and ^{125}I -labeled cholinergic nervemarker (-)-5-iodobenzovesamicol. *Nucl Med Biol* 20:929–937
 - Zea-Ponce Y, Mavel S, Assaad T *et al.* (2005) Synthesis and *in vitro* evaluation of new benzovesamicol analogues as potential imaging probes for the vesicular acetylcholine transporter. *Bioorg Med Chem* 13:745–753